Joint 4-D Visualisation and Analysis of Geodynamic Models and Geological Data

Ömer Faruk Bodur (omer@uow.edu.au)
University of Wollongong
Nicolas Flament
University of Wollongong

Method Article

Keywords:

Posted Date: September 14th, 2022

DOI: https://doi.org/10.21203/rs.3.rs-2047226/v1

Abstract

Advancements in computational methods have shaped investigations of Earth's interior. Geodynamicists model Earth's convective mantle using super-computers, and such complex models create massive outputs that necessitate solutions for effective visualisation and comparison to geological constraints. Here we present an open-source framework for robust 4-D (3-D space and time) joint visualisation of geodynamic models and geological data. The framework brings together geological data and geodynamic models in the same platform allowing for new ways of analysis and more insights on the relationship between Earth's interior and surface. It has applications in both basic research and frontier resource exploration, and is dynamic enough to be used in various applications that require overlapping spatial data over time. In this work, we provide methods and examples to visualise geological data with various geometries in 3-D, showcase applications including mapping Earth's mantle temperature anomalies and chemical composition, tracking materials such as sinking cold mantle structures over time, and using virtual drillholes to probe into Earth's interior for which properties with depth are analysed.

Introduction

Earth resources such as metals are critical for sustainable growth. The quest to find more Earth resources has resulted in a surge of geoscientific data and models. Thanks to the development of information theory (Shannon 1948) which utilized the modernized binary systems (Leibnitz 1703), data can be digitized not only for storage but also for further use in other tools. A recent example of such digitized geoscientific data is age of ocean floor digitized by Müller et al. (1997) used in tectonic plate reconstructions and studying Earth's interior (Müller et al. 2022). Geologists achieved a near complete picture of plate tectonic theory between 1960-1970s, and thanks to advances in computer technology and high-performance computing, seismic tomographic models improved in resolution (Cartwright and Huuse 2005) and geodynamicists created numerical computer simulations of mantle convection to better understand dynamics of Earth's interior (McKenzie et al. 1974). Much effort has been given to provide tools 1/ to visualise geoscientific data and 2/ visualise and analyse outputs of numerical simulations of Earth's interior (Fullsack 1995; Damon et al. 2008; Stegman et al. 2008; Schröder et al. 2012; Kaluza et al. 2019). Such tools are usually focused on visualisation performance, parallel-processing efficiency and visual clarity. Crameri (2018) provided useful routines not only for visualisation but also for diagnosis of dynamics in the convecting mantle in a geodynamic model, and introduced accessible open-access colormaps.

Different properties of geodynamic model outputs can be analysed for different problems. Total normal stress at the surface can be used to predict dynamic topography driven by mantle density anomalies (Flament et al. 2013; Bodur and Rey 2019). Hot mantle structures and mantle plumes can be detected by iso-surfaces of horizontal temperature anomalies (Labrosse 2002; Leng and Gurnis 2012), gradient of radial velocity field (Hassan et al. 2015) or by computing radial heat advection using temperature field and radial velocity (Arnould et al. 2020). In these studies, the detected mantle structures and surface topography were compared against geological constraints (e.g., tectonic subsidence, locations of large

igneous provinces) and geophysical data (e.g., residual topography, seismic tomographic models) which provided insights on the link between surface and Earth's deep interior. Some research questions necessitate extracting properties of geodynamic model output underneath certain geographical locations which varies in geological time (e.g., kimberlite emplacement in the last 200 million years). We are interested in extracting the temperature profile only at reconstructed locations of kimberlite emplacement to determine if kimberlite eruptions are characterised by high heat flow from deep mantle (Torsvik et al. 2010). We also want to visualise reconstructed kimberlites and mantle structures together in the same platform to get insight on overall dynamics in the mantle underneath kimberlites. Likewise, visualising cold mantle structures (i.e., slabs) and tracking subducted slabs over time along with relative positions of cratonic blocks and plate boundaries can also help us in understanding global plate tectonics, positions of mantle structures and their link to continents at the surface (Flament et al. 2022; Müller et al. 2022). We propose that visualising geodynamic model outputs and geoscientific data in the same platform opens new avenues of analysis and robust comparison of geodynamic models against geological constraints. Here, we present an open-source visualisation and analysis framework which makes possible the 4-D joint visualisation and analysis of geoscientific data and geodynamic model output in the same platform. We provide example applications of our framework using CitcomS (Zhong et al. 2008) outputs, but the framework can be adapted for different geodynamic model code outputs. We first discuss how to visualise geological data in open source ParaView software before giving examples of joint visualisation and analysis.

Methodology

4-D Visualisation of Geological Data

Any object or geological feature such as plate boundaries, continents, and data such as kimberlite eruption locations can be represented by VTK (The Visualisation Toolkit) files (www.vtk.org). To visualise a feature, information is required about the locations of points and their connectivity (i.e., geometry) describing how the points are connected in 3D. Objects in VTK consist of points and cells in cartesian coordinates. In our framework, we use the poly-vertex, polyline, unstructured grid and hexahedron linear cell types available in VTK (Fig. 1).

The open-source software GPlates (Müller et al. 2018) makes it possible to develop plate reconstructions and to visualise different sets of geoscientific data. GPlates can render 3D scalar data, color the data with respect to a variable (e.g., depth) unsing built-in color palettes, and apply depth restriction for the visualised data. The visualisation is limited as the camera rotates only around the centre of the globe (i.e., camera tilt is not possible), and data cannot be futher restricted for further analysis through other means such as spatial restrictions in nonradial dimensions or plotting profiles at certain locations such as temperature profile. 2D seismic tomographic depth slices can also be easily visualised using readily accessible map projections in GPlates. For geological data, we use files exported from GPlates (e.g., plate boundaries) or databases (e.g., kimberlite eruptions) that have location (lon, lat) and age (Ma) information. Among the most useful geometries, poly-vertex is a very basic way of representing points

that are not connected in any way (Fig. 1a). Poly-vertex representation is useful for geological features such as kimberlites or the centroid of large igneous provinces. The cells of poly-vertex are defined such that connectivity array attached to the data is comprised of elements of size 1, but the length of the connectivity array must be equal to the length of data or total number of points (i.e., vertexes) to be properly visualised in ParaView. For features represented by poly-lines (e.g., unclosed plate boundaries such as transform, convergent and divergent boundaries), the connectivity array is modified such that consecutive points are connected by lines except the first and last point in the array. In this case, the poly-line is not closed, therefore it cannot be represented as a surface (Fig. 1b). If the polyline is closed, then it becomes a polygon, and a surface is defined for the area covered by the polygon. Multiple polygons come together to form an unstructured grid. Continents can be represented as unstructured grid, which can be directly visualised from a NetCDF file in ParaView. In that case, coordinates of longitude and latitude are automatically converted to cartesian coordinates (Fig. 1c). In ParaView, unstructured grids can be displayed as surfaces. They are also suitable to be viewed as lines and points if desired.

If the data to be visualised consist of points that are significantly far from each other (i.e., > 1,000 km), the lines connecting the vertexes penetrate the Earth surface because vertexes are connected by lines of shortest distance in cartesian geometry, as opposed to great circles in spherical geometry. However, for data such as coastlines or plate boundaries that should be visualised on Earth's surface, the connecting lines should not penetrate into the Earth. To avoid this problem, we increase the sampling rate of the data by interpolating between every consecutive two points through the great circle passing through those two points (Supplementary Information and Connect-Points-Along-Great-Circle.ipynb) because cartesian geometry is an appropriate approximation over small distances.

Analysis of Earth's interior underneath locations of interest can be of useful to Earth scientists. For example, at the kimberlite emplacement locations presented in Fig. 1a, it is possible to query temperature as a function of depth and to visualise virtual drillholes that penetrate to Earth's crust and mantle. These virtual drillholes are hexahedrons that consist of 6 surfaces (Fig. 1d). The bottom (or top) surface are centred on the location of geological data at surface (i.e., kimberlites emplacement locations in Fig. 1a). The size of the bottom and top surfaces is defined as a distance in degrees of longitude and latitude from the geometrical centre of the surface to the walls (spanning parameter in Create-Pseudo-Drillholes-in-ParaView-and-GPlates.ipynb). In the following sections, we will visualise geological data and geodynamic models in the same platform by using VTK in ParaView, and provide examples of how joint analysis can give insights on the link between Earth's interior and surface.

Datasets And Experiments

Dataset Description

In this section, we present a method to post-process and visualise CitcomS 3D spherical geodynamic models (Zhong et al. 2008; Bower et al. 2015; Gurnis et al. 2019) with ParaView, and then present

examples of joint analysis of geodynamic model and geological data (i.e., kimberlite emplacement). We use a modified version of CitcomS (Bower et al., 2015) that is publicly available (https://github.com/EarthByte/citcoms). The standard interface for the code is either a python3 (3.8) code (*.py files) or python3 code written on iPython Notebook (*.ipyn files) for partial execution.

In the CitcomS model we used (i.e., Cases 6 and 7 in Flament et al., 2022) Earth's mantle flow was predicted from 1 billion years ago (Ga) to the present-day. We considered a total of about 13 million computational nodes equally spread over 12 caps, 129 x 129 x 65 nodes in each cap (see next section for the definition of caps), constructed in the spherical coordinates ($\hat{\theta}, \widehat{\varnothing}, \hat{r}$). In the geodynamic model, the computation is based on finite-elements, and mesh resolution increases towards the surface and basal boundaries with a range between 28 km and 50 km in lateral directions ($\hat{\theta}$ and $\widehat{\varnothing}$), and between 27 km and 100 km in radial direction ($\hat{r}$). In the version of CitcomS that we used (Bower et al. 2015), plate motions are imposed at the surface as boundary conditions, synthetic maps of past ocean floor ages (Williams et al. 2021), subduction zone locations as well as their polarities are assimilated over time at 1 Myr intervals. Therefore, the thermal structure of the ocean lithosphere and shallow subduction zones were defined and assimilated. During computation, these constraints are merged with the dynamic solution at every numerical timestep, ensuring that plate subduction is one-sided and that the overriding plate does not subduct. The mantle is considered to be incompressible under the extended-Boussinesq approximation, which considers viscous heat dissipation and the decrease of the coefficient of thermal expansivity with depth. An adiabatic temperature profile is prescribed at the initial age (i.e., 1,000 Ma) with two imposed temperature conditions at the surface and core-mantle boundary (Supplementary Information).

Post-Processing CitcomS Geodynamic Models

For visualisation in Paraview, CitcomS model outputs are converted from spherical ($\hat{\theta}, \widehat{\varnothing}, \hat{r}$) to cartesian coordinates ($\widehat{x}, \hat{y}, \hat{z}$) with unit length ($|r|$ = 1) for Earth's radius. The global, spherical CitcomS shell (1.0 $\geq r \geq$ 0.55) is distributed onto 12 caps with edges oriented diagonally with respect to longitude and latitude (Fig. 2) coordinates.

We use 384 processors to run the model in parallel, therefore the output is distributed across 384 directories. We reassemble the output to create 12 caps per timestep (make_caps.sh), which uses autocombine.py that is distributed with CitcomS (Zhong et al. 2000, 2008; Bower et al. 2015). By default, cap files contain coordinates, velocities, temperature and viscosity, although more fields can be added (written as opt files when optional fields are attached to cap files). OptToVtk.sh creates VTK versions of the cap (or opt) files by following the logic given in Supplementary Information, which is an updated version of the original code released under GNU licence, and developed by Hassan et al., (2015). The code was updated to Pyhton 3.8 and additions were made for the compositional field.

During conversion from spherical to cartesian coordinates, it is essential to preserve the connectivity of points. We use elements of hexahedrons with eight nodes to form cells that represent Earth's interior. The

nodes or vertexes of the hexahedrons as well as their volume depends on the resolution of the model. Mesh refinement in the radial direction can be varied such that the resolution increases towards the surface and core-mantle boundary. OptToVtk.sh creates a *.vtu file for each cap, and Create_PVTUs.sh writes a singular *.pvtu file per timestep which can be opened in ParaView to jointly read 12 caps (*vtu files) visualise the entire globe. With 12 processors for the visualisation, ParaView distributes the data to 12 processors (> 1 million points per processor, which is the recommended upper limit). This is important for efficiency in interactive visualisation and prompt response of ParaView built-in filters during the analysis.

In ParaView, the Annotate Time Filter can be used to create timestamps and attribute ages to each timestep in a sequence of *pvtu files by providing an initial time (e.g., 1000 Ma) and increment (e.g., 20 Myr). Temperature_Anomaly data are contoured to represent hot and cold mantle structures. For cold mantle structures, we first clip the data for depths greater than 300 km to avoid visualising the (assimilated) lithosphere and to see through the surface and show deep slabs. After clipping, we contour the data at Temperature_Anomaly iso-value − 0.05, corresponding to 155 K colder than ambient mantle as shown in Fig. 3, coloured by depth in cold colours. For hot mantle structures, we create another clip in the ParaView pipeline and constrain the depths between 170 km and the core-mantle boundary (~ 2,867 km). After clipping, we contour Temperature_Anomaly data at iso-value 0.1, corresponding to 310 K hotter than ambient mantle shown in Fig. 3, coloured by depth in warm colours. To represent Earth's surface and provide a fixed reference frame for the mantle structures, we depict graticules at 60° increment in longitude (0°, 60°, 120°, 180°, 240°) and 30° increment in longitude (-60°, -30°, 0°, 30°, 60°) by using code Create-Graticules-in-ParaView.ipynb. The increments and the resolution of the graticules can be changed accordingly.

Sampling the Mantle Along Virtual Drillholes

Virtual drillholes make it possible to extract mantle properties at depth from a geodynamic model. The tool can be useful across scales in frontier resource exploration because it can provides localised analysis at desired geographical locations. When used in global geodynamic models, they can give insight on investigations of deep reservoir targets (Archer et al. 2005; Cartwright and Huuse 2005) and support more informed decision (Witter and Phillips 2012; Witter and Melosh 2018). To compare the mantle structures with geological constraints, we need to load both the geodynamic model and geological data to ParaView. As an example, we use kimberlite emplacement location and age data (Tappe et al. 2018) sampled within 10 Myr of their emplacement age and visualised in 20 Myr increments to match the resolution of the geodynamic model. We reconstruct kimberlites locations based on their age and present-day location using PyGPlates (Williams et al. 2017) and a plate reconstruction model (Merdith et al. 2021). After reconstructing the kimberlites (Create-Pseudo-Drillholes-in-ParaView-and-GPlates.ipynb), we save their locations at a given time in arrays and write them as VTK hexahedron files by using Meshio python package (https://pypi.org/project/meshio/). After setting a buffer to determine the size of bottom and top cells of hexahedrons, we save it as VTK files describing hexahedrons extending from the surface to the core-mantle boundary. We show virtual drillholes at kimberlite

emplacement locations reconstructed at 180 Ma, along with deep mantle structures and reconstructed continents at the surface (Fig. 4). It is also possible to convert virtual drillholes in VTK format to grid files to visualise in GPlates (Supplementary Information and Create-Pseudo-Drillholes-in-ParaView-and-GPlates.ipynb).

We are interested in the temperature field underneath kimberlite locations, which we can extract by resampling the virtual drillholes with the temperature field output from the geodynamic model by using “Resample Data” filter in ParaView. We plot the average temperature along the drillholes extending from the surface of the Earth to the core-mantle boundary (Fig. 5). We compare the calculated profile with the horizontal averaged temperature profile of the global geoydnamic model at 180 Ma (grey line in Fig. 5). The average temperature field beneath kimberlites shows slightly higher temperatures in the shallow mantle and mid-mantle. This implis that both deep and shallow mantle dynamics could be important to understand the heat flow underneath kimberlites.

Analysing the Composition Field

CitcomS geodynamic models can include compositionally distinct elements (e.g., continental crust, basal layer) at the onset on of the model run (i.e., 1,000 Ma) (McNamara and Zhong 2004). This makes it possible to consider density differences that cannot be attributed to changes in temperature. The composition field is described by tracers which advect using a predictor-corrector method (McNamara and Zhong 2004). We keep track of the composition via the tracer ratio method (Tackley and King 2003), giving percentage of tracers for each computational element, which allows for visualising compositional mixing in the mantle.

In this example, we are interested in how much continental crust is recycled to the mantle because there are indications for geochemical signature of continental crust in flood basalts in African hemisphere rather than the Pacific. We want to see if assimilated subduction in CitcomS models result in crustal mixture to the mantle and explain geochemical observations (Doucet et al. 2020). We show the computational elements that consist of at least 5% of tracers coming from the continental crust at present for Case 7 of Flament et al. (2022) (Fig. 6). We use cold colours to indicate depth for continental crust tracers. This reveals that the mantle underneath Africa (Fig. 6b) contains more recycled continental crust than the mantle underneath the Pacific Ocean (Fig. 6a), which is consistent with the isotopic geochemical dichotomy (i.e., Pb, Nd and Sr) of plume induced basalts above each basal mantle structure (Doucet et al. 2020).

Particle Tracking in ParaView

In CitcomS geodynamic models, plates subduct along subduction boundaries and sink deep into the mantle. Model processing is required to understand the complex interactions between slabs and hot mantle structures. We use the ParaView “Particle Tracer Filter” to determine the path of slabs over time from the time-dependent velocity field. This filter requires seed points that are advected forward in time. As in Flament et al. (2022), we considered seeds as a single VTK file with polyvertex data located within slabs at ~ 250 km depth at 740 Ma (Fig. 7). These seeds were filtered to select those that sink deep and

interact with very deep hot mantle structures. The calculation from the Particle Tracer Filter needs to be scaled by because outputs was written at 20 Myr increment. The scaling is done by calculating the nondimensional factor for 20 Myr time interval as follows:

$t' = \frac{t\kappa_0}{{R_0}^2}$ (1),

which with time t = 20 Myr, the reference thermal diffusivity κ_0 = $10^{-6}m^2s^{-1}$, and Earth's radius R_0 = 6,371 km, yields ascaling factor t' = $1.554x10^{-5}$.

Discussion

Tools built to visualise and analyse geodynamic model make it possible to gain insights into the interaction between Earth's surface and convection in the mantle. Analysing a geodynamic model is important considering the time, effort and computational source required in creating them. Significant efforts have been dedicated to the post-processing and analysis of geodynamic models. For example, StagLab provided methods for visualisation of geodynamic model outputs, especially for StagYY geodynamic modelling code (Tackley 2008), and provides useful routines for effective analysis (Crameri 2018), similar to ADOPT (Mallard et al. 2017) which was built to detect some important features in geodynamic model outputs such as plate boundaries. Others have contributed to the evolving geodynamic model visaulisation tools by improving the effective visalisation technology for better analysis and understanding (Damon et al. 2008), whereas some geodynamic modelling codes (e.g., Underworld (Moresi et al. 2003, 2007) and ASPECT (Kronbichler et al. 2012)) adapted output formats suitable to visualise in ParaView software (Ahrens et al. 2005) to make use of ParaView's capabilities in geodynamic model output visualisation and analysis. The field has developed to the extent that immersive visualisation of geodynamic models for better user experience and interactive visualisation and analysis is now possible (Billen et al. 2008; Wiedemann et al. 2015; Jadamec 2016; Rey 2022). The software package gLucifer, makes 'on-the-fly' visualisation possible, and it does not require writing data to disk (Stegman et al. 2008). This functionality makes it possible for users to efficiently and easily visualise large geodynamic models, which is a common problems in geodynamic modelling. A limit of 'on-the-fly' visualisation is the reduction of freedom in model output visualisation and analysis because the properties and parts of the model to be visualised need to be declared before running the geodynamic model. However, this can be overcome by traditional way of visualisation, which is properly checkpointing the model run, and restarting it from the last checkpoint for the desired visualisation.

Independent from improvements on geodynamic visualisation tools, Earth scientists who collect or work with geoscientific data such as seismic tomography, have benefited from improvements in technology (e.g., 3-D seismic technology (Cartwright and Huuse 2005; Witter and Melosh 2018)). GPlates, which was built for using digitized geoscientific data and reconstructing plates back in time, makes it possible to visualise global geoscientific datasets such as tomographic and mantle flow models in 3-D, and more recently, the GPlates portal was built for fast and interactive visualisation through a web portal (Müller et al. 2016). Submachine is another useful free web-based service built for visualisation and quantitative

analysis of seismic tomographic models and other geophysical data (Hosseini et al. 2018). Python package PVGeo provides visualisation and integration of geoscientific data, and uses VTK libraries and ParaView software (Sullivan and Trainor-Guitton 2019).

Geodynamic model outputs and geoscientific data have hitherto been visualised and compared in separate platforms (e.g., Burgess and Gurnis, 1995; Flament et al., 2013; Mondy et al., 2018; Şengül Uluocak et al., 2021). Our framework brings them together. We showed that useful information can be derived from 4-D joint visualisation and analysis of geodynamic models and geoscientific data in the same platform. We also show that this can be done efficiently using Python libraries and open source ParaView software. Using VTK libraries also allowed to do analysis in new ways such that we created virtual drillholes and sampled the properties of Earth's mantle in a geodynamic model.

There are avenues for improvement in our framework. For example, the data processing and visualisation in ParaView is currently done through a sequential pipeline (see discussion at https://www.kitware.com/scientific-visualization-in-2022/). When a filter is busy with executing, rendering is stopped until the filter finalises the execution. For computationally-heavy tasks such as particle tracking in a large geodynamic model, choosing the correct seeds and analysing particle paths require significant time. In the future, these tasks may be done more efficiently if data processing in ParaView could be done through concurrent pipelines which may allow partial or full visualisation of the result during execution. Furthermore, grid computing may also be implemented in the future (Brodlie et al. 2004; Stegman et al. 2008) to support performance in visualisation of massive geodynamic models.

Conclusion

Using currently available tools which are all open-access, we provided a framework with explanations on how to creatively visualise and analyse geological data and geodynamic models by using open-source tools. The framework brings together geological data and geodynamic models in the same platform allowing for new ways of analysis. It aims to give more insight on the relationship between Earth's interior and surface. It has applications in frontier resource exploration and basic research, and can be adapted for use in other applications that necessitate analysis of overlapping data in space and time.

Declarations

Competing Interests: The authors have no relevant financial or non-financial interests to disclose.

Funding ÖFB and NF were supported by Australian Research Council grant LP170100863 (industry partner: De Beers). This research was undertaken with the assistance of resources from the National Computational Infrastructure (NCI), which is supported by the Australian Government. Access to NCI was partly supported by resources and services from the University of Wollongong (UOW).

Author contributions (CRediT author statement) Ömer F. Bodur: Conceptualization, Methodology, Software, Validation, Formal Analysis, Investigation, Writing – Original Draft, Visualization. **Nicolas**

Flament: Conceptualization, Methodology, Validation, Writing – Review & Editing, Resources, Project Administration, Funding Acquisition.

Code availability This framework is built on existing codes, the original authors of which have been indicated in the header of each file, therefore our framework includes codes that are modified as precisely defined in GNU General Public Licence 3 published by the Free Software Foundation. All files and codes can be accessed at https://github.com/ofbodur/Joint-4D-Visualisation-and-Analysis-of-Geodynamic-Models-and-Geological-Data.

References

1. Ahrens J, Geveci B, Law C (2005) Paraview: An end-user tool for large data visualization.Vis Handb717
2. Archer SG, Bergman SC, Iliffe J et al (2005) Palaeogene igneous rocks reveal new insights into the geodynamic evolution and petroleum potential of the Rockall Trough, NE Atlantic Margin. Basin Res 17:171–201
3. Arnould M, Coltice N, Flament N, Mallard C (2020) Plate tectonics and mantle controls on plume dynamics. Earth Planet Sci Lett 547:116439. https://doi.org/10.1016/j.epsl.2020.116439
4. Billen MI, Kreylos O, Hamann B et al (2008) A geoscience perspective on immersive 3D gridded data visualization. Comput Geosci 34:1056–1072. https://doi.org/https://doi.org/10.1016/j.cageo.2007.11.009
5. Bodur ÖF, Rey PF (2019) The impact of rheological uncertainty on dynamic topography predictions. Solid Earth 10:2167–2178. https://doi.org/10.5194/se-10-2167-2019
6. Bower DJ, Gurnis M, Flament N (2015) Assimilating lithosphere and slab history in 4-D Earth models. Phys Earth Planet Inter 238:8–22. https://doi.org/https://doi.org/10.1016/j.pepi.2014.10.013
7. Brodlie K, Duce J, Gallop J et al (2004) Visualization in grid computing environments. In: IEEE Visualization 2004. pp 155–162
8. Burgess PM, Gurnis M (1995) Mechanisms for the formation of cratonic stratigraphic sequences. Earth Planet Sci Lett 136:647–663. https://doi.org/10.1016/0012-821X(95)00204-P
9. Cartwright J, Huuse M (2005) 3D seismic technology: the geological 'Hubble'. Basin Res 17:1–20
10. Crameri F (2018) Geodynamic diagnostics, scientific visualisation and StagLab 3.0. Geosci Model Dev 11:2541–2562. https://doi.org/10.5194/gmd-11-2541-2018
11. Damon M, Kameyama MC, Knox M et al (2008) Interactive visualization of 3D mantle convection. Vis Geosci 13:49–57. https://doi.org/10.1007/s10069-007-0008-1
12. Doucet LS, Li Z-X, Gamal El Dien H et al (2020) Distinct formation history for deep-mantle domains reflected in geochemical differences. Nat Geosci 13:511–515. https://doi.org/10.1038/s41561-020-0599-9

13. Flament N, Bodur ÖF, Williams SE, Merdith AS (2022) Assembly of the basal mantle structure beneath Africa. Nature 603:846–851
14. Flament N, Gurnis M, Müller RD (2013) A review of observations and models of dynamic topography. Lithosphere 5:189–210. https://doi.org/10.1130/L245.1
15. Fullsack P (1995) An arbitrary Lagrangian-Eulerian formulation for creeping flows and its application in tectonic models. Geophys J Int 120:1–23. https://doi.org/10.1111/j.1365-246X.1995.tb05908.x
16. Gurnis M, Bower DJ, Turner M et al (2019) Creating 4-D Earth models using GPlates. CitcomS and the Geodynamic Framework
17. Hassan R, Flament N, Gurnis M et al (2015) Provenance of plumes in global convection models. Geochem Geophys Geosyst 16:1465–1489
18. Hosseini K, Matthews KJ, Sigloch K et al (2018) SubMachine: Web-based tools for exploring seismic tomography and other models of Earth's deep interior. Geochem Geophys Geosyst 19:1464–1483
19. Jadamec MA (2016) Insights on slab-driven mantle flow from advances in three-dimensional modelling. J Geodyn 100:51–70. https://doi.org/https://doi.org/10.1016/j.jog.2016.07.004
20. Kaluza OL, Moresi L, Mansour J et al (2019) LavaVu
21. Kronbichler M, Heister T, Bangerth W (2012) High accuracy mantle convection simulation through modern numerical methods N3–10.1111/j.1365-246X.2012.05609.x. Geophys. J. Int
22. Labrosse S (2002) Hotspots, mantle plumes and core heat loss. Earth Planet Sci Lett 199:147–156. https://doi.org/https://doi.org/10.1016/S0012-821X(02)00537-X
23. Leibnitz G-G (1703) Explication de l'arithmétique binaire, qui se sert des seuls caracteres O et I avec des remarques sur son utilité et sur ce qu'elle donne le sens des anciennes figures chinoises de Fohy. Hist l'Académie R des Sci avec les mémoires Académie des Sci
24. Leng W, Gurnis M (2012) Shape of thermal plumes in a compressible mantle with depth-dependent viscosity.Geophys Res Lett39
25. Mallard C, Jacquet B, Coltice N (2017) ADOPT: A tool for automatic detection of tectonic plates at the surface of convection models. Geochem Geophys Geosyst 18:3197–3208
26. McKenzie DP, Roberts JM, Weiss NO (1974) Convection in the Earth's mantle: towards a numerical simulation. J Fluid Mech 62:465–538
27. McNamara AK, Zhong S (2004) Thermochemical structures within a spherical mantle: Superplumes or piles?J Geophys Res Solid Earth109
28. Merdith AS, Williams SE, Collins AS et al (2021) Extending full-plate tectonic models into deep time: Linking the Neoproterozoic and the Phanerozoic. Earth Sci Rev 214:103477. https://doi.org/https://doi.org/10.1016/j.earscirev.2020.103477
29. Mondy LS, Rey PF, Duclaux G, Moresi L (2018) The role of asthenospheric flow during rift propagation and breakup. Geology 46:103–106. https://doi.org/10.1130/G39674.1
30. Moresi L, Dufour F, Mühlhaus H-B (2003) A Lagrangian integration point finite element method for large deformation modeling of viscoelastic geomaterials. J Comput Phys 184:476–497.

https://doi.org/10.1016/S0021-9991(02)00031-1

31. Moresi L, Quenette S, Lemiale V et al (2007) Computational approaches to studying non-linear dynamics of the crust and mantle. Phys Earth Planet Inter 163:69–82. https://doi.org/10.1016/j.pepi.2007.06.009
32. Müller RD, Cannon J, Qin X et al (2018) GPlates: building a virtual Earth through deep time. Geochem Geophys Geosyst 19:2243–2261
33. Müller RD, Cannon J, Tetley M et al (2022) A tectonic-rules based mantle reference frame since 1 billion years ago–implications for supercontinent cycles and plate-mantle system evolution.Solid Earth Discuss1–42
34. Müller RD, Qin X, Sandwell DT et al (2016) The GPlates portal: Cloud-based interactive 3D visualization of global geophysical and geological data in a web browser. PLoS ONE 11:e0150883
35. Müller RD, Roest WR, Royer J et al (1997) Digital isochrons of the world's ocean floor. J Geophys Res Solid Earth 102:3211–3214
36. Rey P (2022) Geological mapping in an immersive virtual world: A proof of concept. Copernicus Meetings
37. Schröder S, Peterson JA, Obermaier H et al (2012) Visualization of Flow Behavior in Earth Mantle Convection. IEEE Trans Vis Comput Graph 18:2198–2207
38. Şengül Uluocak E, Göğüş OH, Pysklywec RN, Chen B (2021) Geodynamics of East Anatolia-Caucasus Domain: Inferences From 3D Thermo-Mechanical Models, Residual Topography, and Admittance Function Analyses. Tectonics 40:e2021TC007031
39. Shannon CE (1948) A mathematical theory of communication. Bell Syst Tech J 27:379–423. https://doi.org/10.1002/j.1538-7305.1948.tb01338.x
40. Stegman DR, Moresi L, Turnbull R et al (2008) gLucifer: next generation visualization framework for high-performance computational geodynamics. Vis Geosci 13:71–84
41. Sullivan CB, Trainor-Guitton WJ (2019) PVGeo: an open-source Python package for geoscientific visualization in VTK and ParaView. J Open Source Softw 4:1451
42. Tackley PJ (2008) Modelling compressible mantle convection with large viscosity contrasts in a three-dimensional spherical shell using the yin-yang grid. Phys Earth Planet Inter 171:7–18. https://doi.org/https://doi.org/10.1016/j.pepi.2008.08.005
43. Tackley PJ, King SD (2003) Testing the tracer ratio method for modeling active compositional fields in mantle convection simulations.Geochemistry, Geophys Geosystems4
44. Tappe S, Smart K, Torsvik T et al (2018) Geodynamics of kimberlites on a cooling Earth: Clues to plate tectonic evolution and deep volatile cycles. Earth Planet Sci Lett 484:1–14. https://doi.org/10.1016/j.epsl.2017.12.013
45. Torsvik TH, Burke K, Steinberger B et al (2010) Diamonds sampled by plumes from the core-mantle boundary. Nature 466:352–355. https://doi.org/10.1038/nature09216

46. Wiedemann M, Anthes C, Bunge H-P et al (2015) Transforming Geodata for Immersive Visualisation. In: 2015 IEEE 11th International Conference on e-Science. IEEE, pp 249–254
47. Williams S, Cannon J, Qin X, Müller D (2017) PyGPlates-a GPlates Python library for data analysis through space and deep geological time. In: EGU General Assembly Conference Abstracts. p 8556
48. Williams S, Wright NM, Cannon J et al (2021) Reconstructing seafloor age distributions in lost ocean basins. Geosci Front 12:769–780
49. Witter JB, Melosh G (2018) The Value and Limitations of 3D Models for Geothermal Exploration. 43rd Work Geotherm Reserv Eng Stanford Univ SGP-TR-213
50. Witter JD, Phillips N (2012) Integrated 3D geophysical inversion and geological modelling for improved geothermal exploration and drillhole targeting. GRC Trans 36:831–834
51. Zhong S, McNamara A, Tan E et al (2008) A benchmark study on mantle convection in a 3-D spherical shell using CitcomS. Geochem Geophys Geosyst 9. https://doi.org/10.1029/2008GC002048
52. Zhong S, Zuber MT, Moresi L, Gurnis M (2000) Role of temperature-dependent viscosity and surface plates in spherical shell models of mantle convection. J Geophys Res Solid Earth 105:11063–11082

Figures

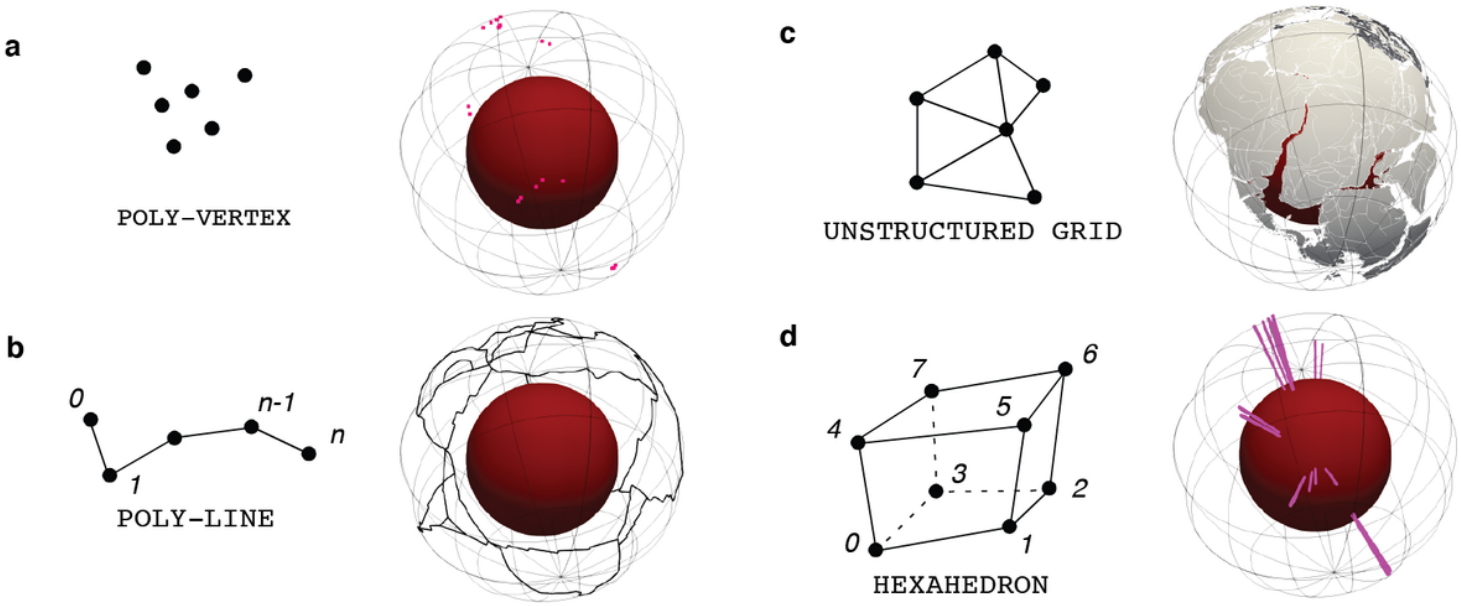

Figure 1

Linear cell types used to represent data in 3-D in this study. a Kimberlite emplacement reconstructed at 180 Ma are shown in poly-vertex form. **b** Plate boundaries reconstructed at 180 Ma and shown as poly-lines. **c** Continents reconstructed at 180 Ma shown as shaded surface of an unstructured grid. **d**Kimberlites reconstructed at 180 Ma, shown as virtual drillholes in hexahedron forms extending from eruption location at the surface to the core-mantle boundary (red sphere).

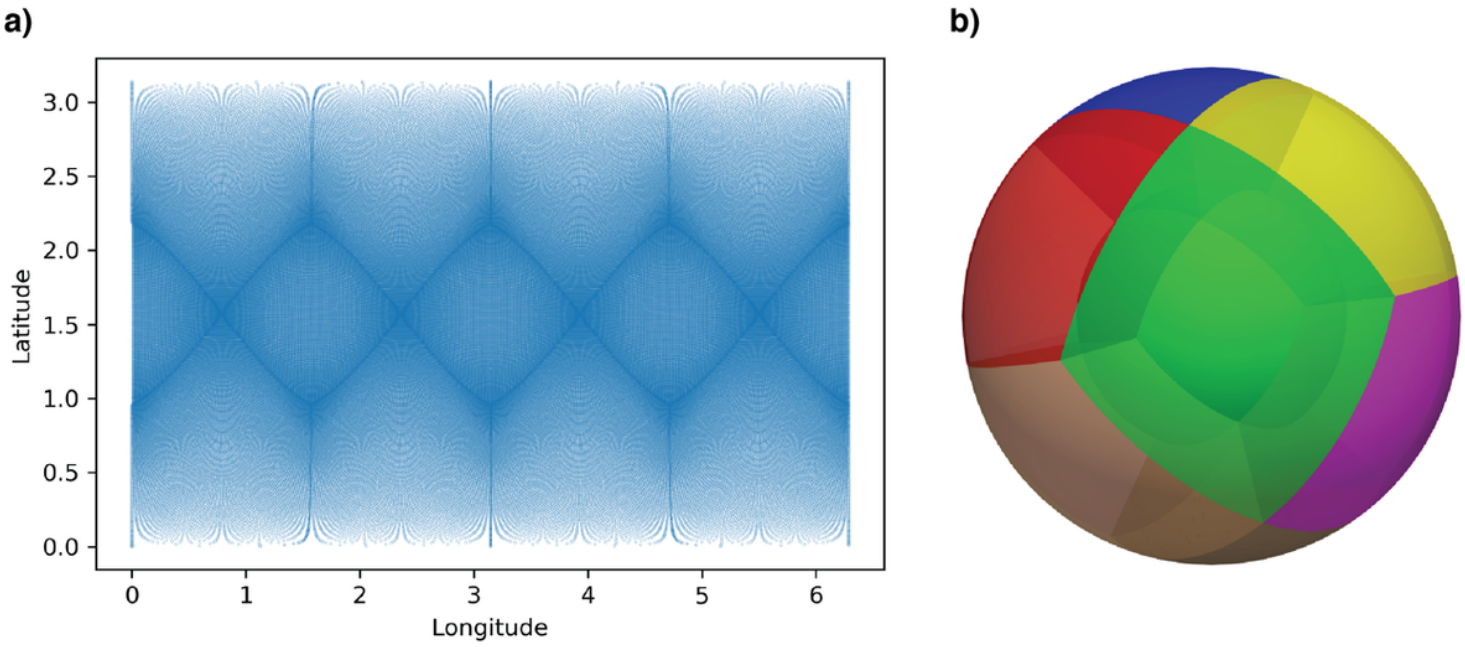

Figure 2

Topology of the global CitcomS mesh. The 3-D spherical geometry in CitcomS was introduced in Zhong et al. (2000). **a**Vertexes are constructed based on desired resolution and are distributed over 12 caps, **b** for parallel computing as well as postprocessing. The latitude and longitude are shown in radians. The caps communicate through boundaries in between (e.g., ghost cells) as can be seen from the increased density of points in **a**.

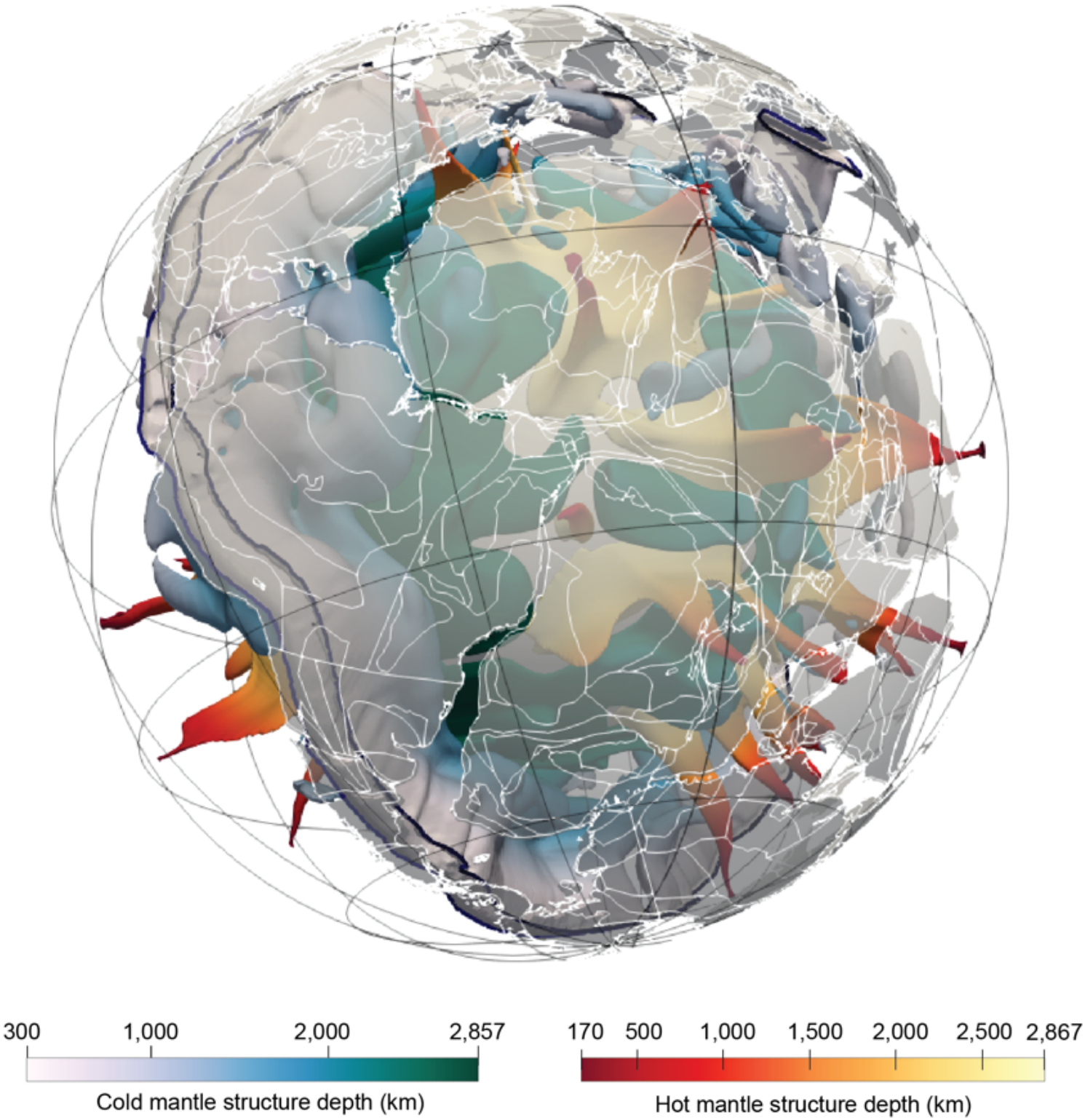

Figure 3

A snapshot of 3D Visualisation of CitcomS geodynamic model output for Case 6 in Flament et al. (2022), at 180 Ma. Hot mantle structures defined by 310 K warmer than ambient mantle below 170 km depth coloured by depth using warm colours, and cold mantle structures 155 K colder than ambient mantle coloured by depth using cold colours. Virtual drillholes (pink hexahedrons) are shown at reconstructed

kimberlites emplacement locations. Reconstructed continents are shown in grey, and geological boundaries and coastlines are shown as white polylines.

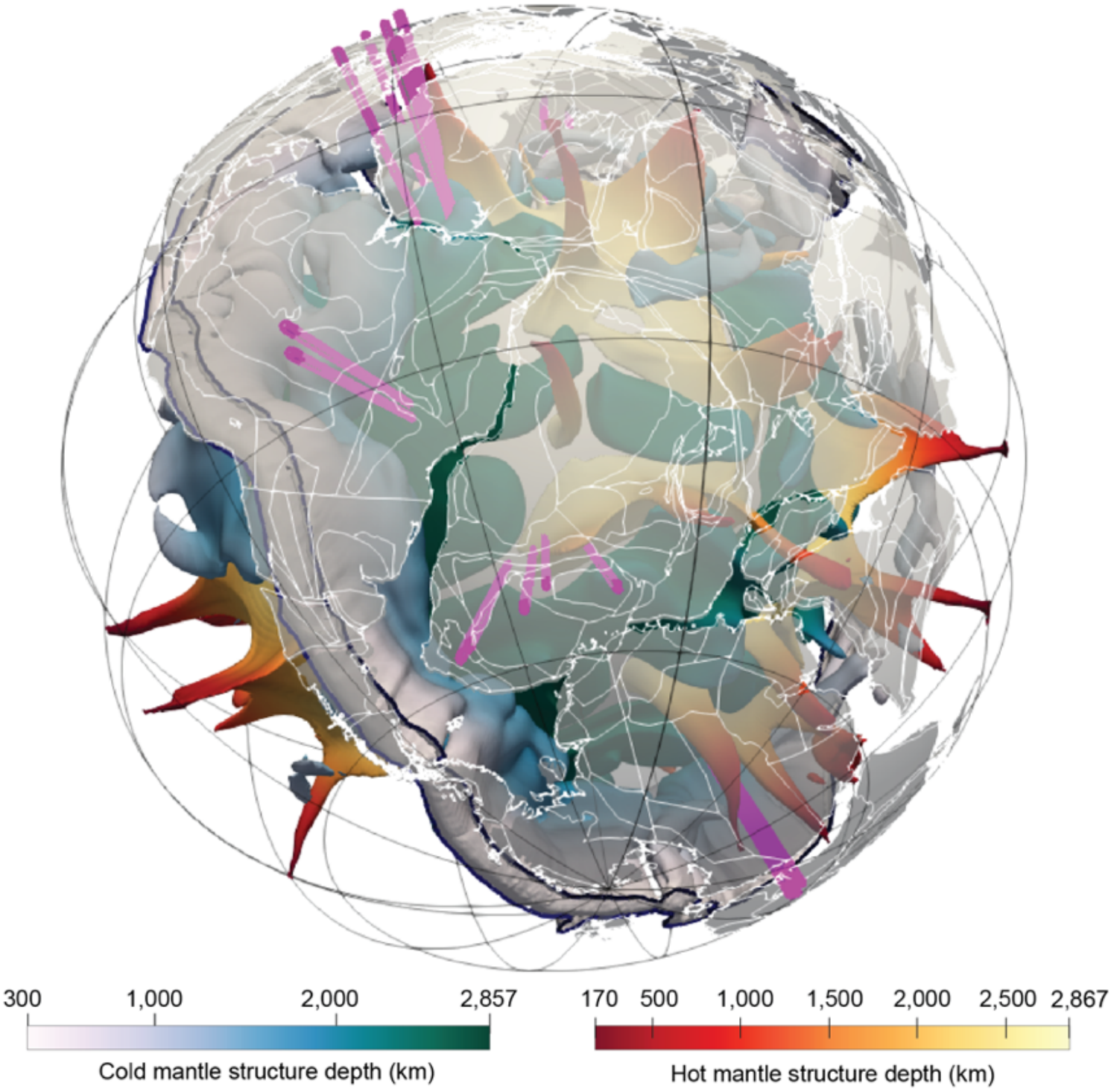

Figure 4

Same as Figure 3, but including virtual drillholes (shown as magenta hexahedrons) at locations of reconstructed kimberlites at 180 Ma.

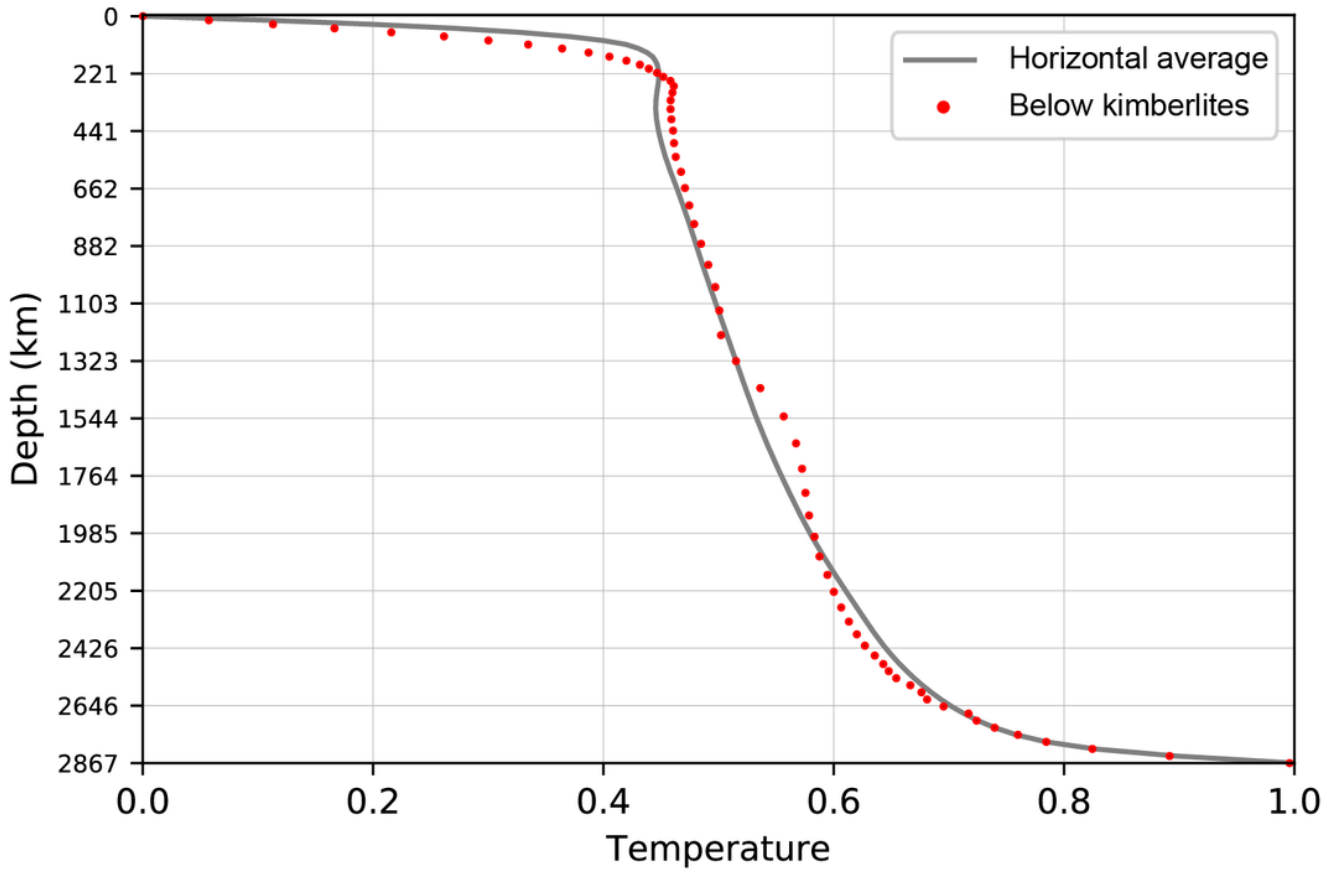

Figure 5

Average temperature profile underneath reconstructed kimberlites at 180 Ma. The temperature profile underneath kimberlites (red dots) are calculated along virtual drillholes shown in Figure 4 and compared with horizontal average temperature at 180 Ma.

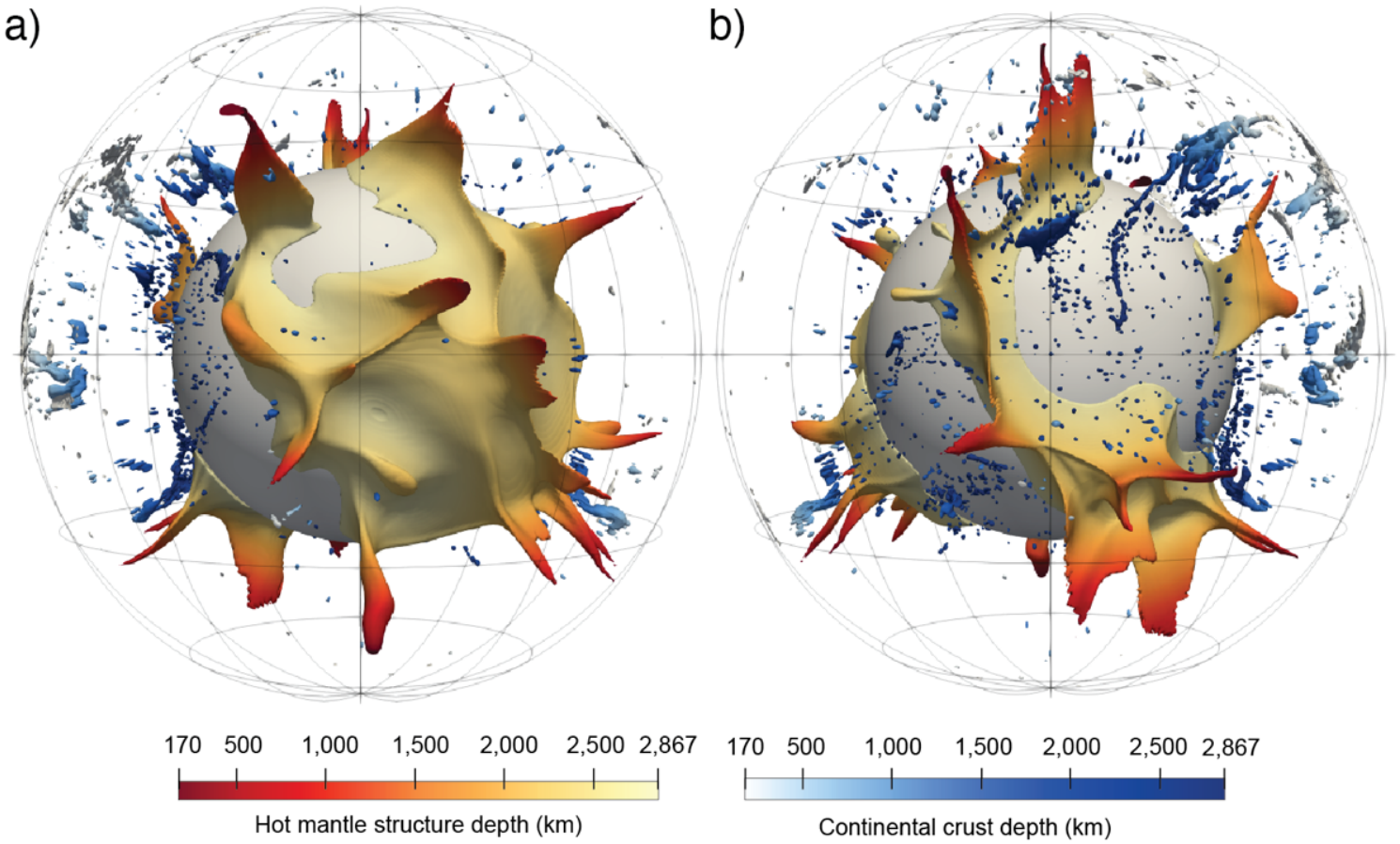

Figure 6

Predicted continental crust mixing in the mantle. Hot mantle structures are shown in warm colours, continental crust consisting of at least 5% is shown for depths below 170 km, coloured by depth with cold colours for the **a** Pacific mantle domain and **b** African mantle domain (modified from Flament et al., 2022)

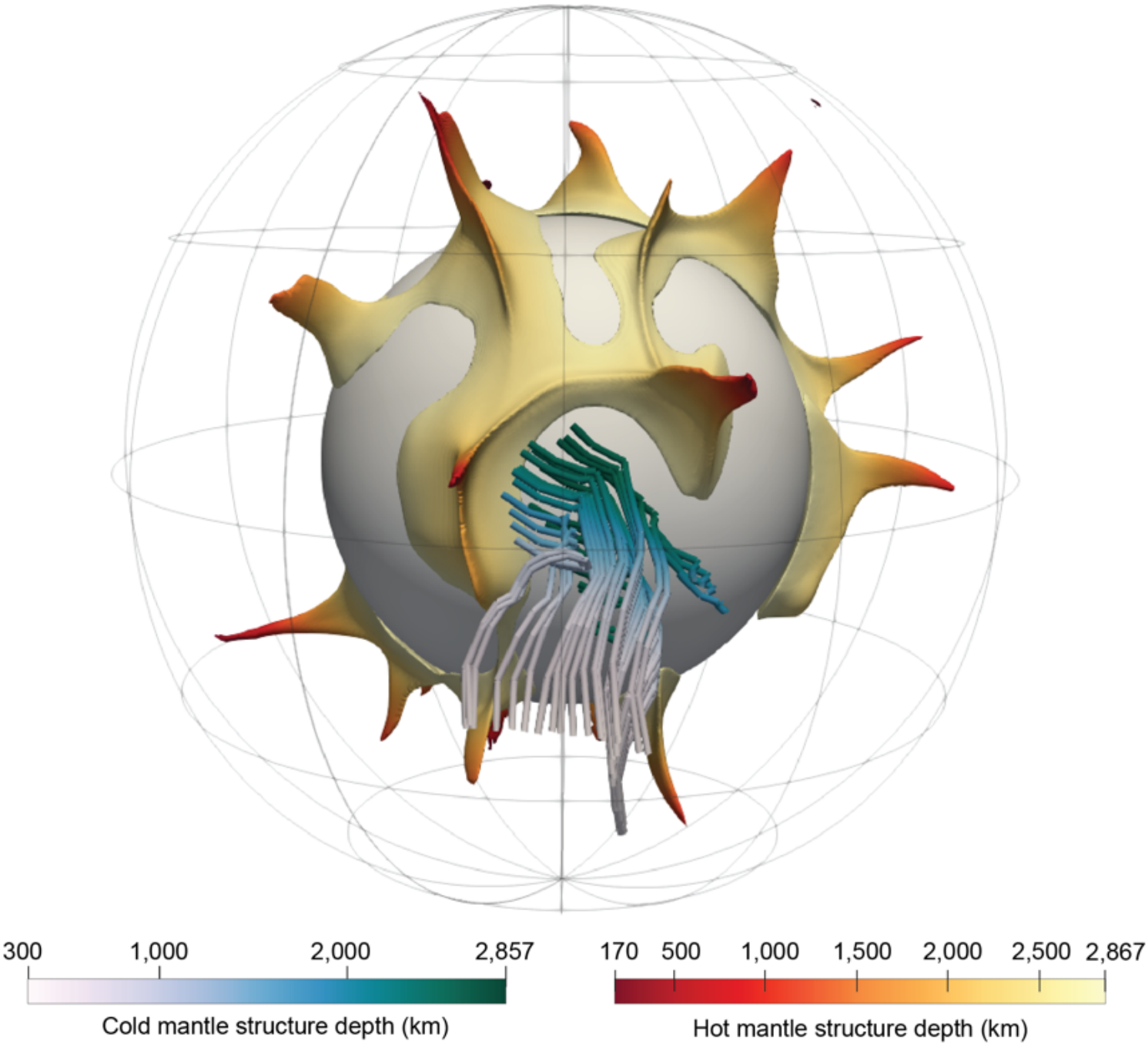

Figure 7

A 240-Myr slab trail between 740 Ma and 500 Ma, coloured by depth similar to cold mantle structures in Fig. 3, modified from (Flament et al. 2022). The trails show subducted slabs that reached the deep mantle, pushing hot mantle structures.

Supplementary Files

This is a list of supplementary files associated with this preprint. Click to download.

- BodurandFlamentSupplementaryInformation9September2022.docx